J. Membrane Biol. 45, 293-310 (1979)

Distribution of Potassium and Chloride Permeability over the Surface and T-Tubule Membranes of Mammalian Skeletal Muscle

Angela F. Dulhunty

Department of Anatomy, University of Sydney, 2006, Australia

Received 30 June 1978

Summary. The distribution of K and Cl permeability, P_K and P_{Cl}, over the surface and T-tubule membranes of red rat sternomastoid fibers has been determined. Membrane potential, V_m, was recorded with 3-M KCl-filled glass microelectrodes. Changes in V_m with changes in $[K]_o$ or $[Cl]_o$ were used to estimate P_{Cl}/P_K in normal and detubulated preparations. The results show that the T-tubule membrane has a high P_{Cl} and is therefore different from the T-tubule membrane of amphibian fibers. Analysis of the time course of depolarization when $[K]_o$ was raised (in SO_4 solutions) showed that P_K was distributed over the surface and T-tubule membranes. Two observations suggested that T-tubule P_{Cl} was higher than the surface P_{Cl}. Firstly, in normal fibers, the depolarization caused by an increase in $[K]_o$ was 3.5 times greater in SO_4 solutions than in Cl solutions. In marked contrast, the depolarization in glycerol-treated fibers was independent of $[Cl]_o$. Secondly, the rapid change in V_m when $[Cl]_o$ was changed was reduced by 80% after glycerol treatment. Both observations suggest that P_{Cl} was low in glycerol-treated fibers. P_{Cl}/P_K was calculated from the V_m data using Goldman, Hodgkin and Katz equations for Na and K or for Na, K, and Cl. In normal fibers $P_{Cl}/P_K = 4.5$ and in glycerol-treated fibers $P_{Cl}/P_K = 0.28$. Since it is unlikely that glycerol treatment would increase P_K, the reduction in the ratio must follow the loss of Cl permeability "channels" in the T-tubule membrane.

The plasmalemma of skeletal muscle fibers can be structurally and functionally divided into two parts, an exterior surface or surface component and a T-tubule component. Knowledge of the distribution of passive conductances over the two membrane areas helps in understanding their electrical properties, including propagation of the action potential (*see*, e.g., Adrian *et al.*, 1970). It has become apparent that the specific conductances of the surface and T-tubule membranes can be different and that the ions carrying current across the membrane can be different. The surface membrane of frog semitendinosus and sartorius muscle fibers has a high Cl conductance, G_{Cl}, while the T-tubule membrane has a very low G_{Cl} (Hodgkin & Horowicz, 1960; Eisenberg & Gage, 1969). It is uncertain whether the density of conductance "channels" can differ between the two membranes or whether there is a restriction on the entry of Cl ions into the T-tubule lumen. The observation that the G_{Cl} of the T-tubule membrane of rat diaphragm fibers is greater than that of amphibian fibers (Palade & Barchi, 1977) is relevant

0022-2631/79/0045-0293 $03.60

to this question. It seems unlikely that a phenomenon responsible for excluding Cl ions from the T-tubules of one species would be absent or act, in fact, to accumulate Cl ions in the T-tubules of a second species.

The experiments in this paper were undertaken to see whether the observation on the rat diaphragm could be repeated in another mammalian skeletal muscle since the diaphragm has been shown to have certain unique properties in other respects (Dulhunty, 1978*a*). Relative Cl and K permeability, P_{Cl}/P_K was determined from the changes in membrane potential, V_m, caused by changes in the external concentrations of K and Cl ions, $[K]_o$ and $[Cl]_o$, respectively. The results show that the distribution of P_{Cl} in red rat sternomastoid fibers is similar to that reported for rat diaphragm and different from that reported for amphibian fibers. The specific G_{Cl} of the T-tubule membrane is higher than that of the surface membrane so that the apparent distribution of conductances is unlikely to be due to difference between Cl concentration in the T-tubule lumen and that outside the surface membrane.

Some of these results have been reported briefly elsewhere (Dulhunty, 1978*b*).

Materials and Methods

Experiments were performed on surface fibers of small bundles (approx. .01 cm^2) dissected from the red segment of sternomastoid muscles from adult male Wistar rats. The bundle was dissected at room temperature and mounted in a small volume bath through which flowed oxygenated Krebs at 37°C. The exchange time for the bath at maximum flow rates was 1 sec. The solutions used are listed in Table 1. Tetrodotoxin, 1×10^{-7} g/ml (Calbiochem, USA), was used to stop regenerative activity and Dantrolene, 1×10^{-4} g/ml (Smith, Kline & French, Australia), was used to reduce contractures in low $[Cl]_o$ solutions (Adrian & Bryant, 1974).

Glycerol Treatment

Glycerol treatment using 400 mM glycerol-Krebs solution had a particularly destructive effect on red sternomastoid fibers. The results could not be improved by reducing the tem-

Table 1. Solutions

Solution	Ion concentration (mM)					Sucrose (mM)	Osmolality	Ionic strength
	Na	K	Ca	Cl	SO_4			
A	150	3.5	2.5	160	—	—	329	163
B	103.5	50	2.5	156.5	—	—	325.5	163
C	84	3.5	6.0	8	46.75	168.75	330	156.3
D	37.5	50	6.0	8	46.75	168.75	330	156.3
E	126.0	3.5	6.0	8	67.75	253.13	477.5	219.3
F	79.5	50	6.0	8	67.75	253.13	477.5	219.3

NB: In addition all solutions contained (in mM): glucose, 11; Mg, 1.0; and Hepes, 1 (pH 7.4).

perature to 24°C or by increasing the divalent cation concentration of the Krebs solution used after exposure to the glycerol solution (Eisenberg, Howell & Vaughan, 1971). The surface fibers appeared to be broken and had low resting V_m values. The condition of the fibers did improve when lower concentrations of glycerol were used. Table 2 lists the average V_m recorded 30 min to 2 hr after treatment with 200, 300, 350, and 400 mM glycerol. The highest average V_m was recorded after treatment with 200 mM glycerol; however, mechanical activity could often be recorded from these fibers, and the continuity of the T-system was unknown. A few surface fibers with V_m greater than −65 mV and with no apparent mechanical activity could be found after treatment with 350 or 400 mM glycerol, and these fibers were used in the experiments reported in *Results*.

Theoretical

The time course of V_m changes following a change in $[K]_o$ with SO_4 as the principal external anion was calculated in the following way. As a first approximation the membrane was treated as a plane sheet at a constant distance 1 from the well-stirred bulk solution. $[K]_m$, the concentration of K at the membrane, was calculated at time t after a change in $[K]_o$, (*see*, e.g., Crank, 1975).

$$[K]_m = [K]_0 + \frac{4[K]_0}{\pi} \sum_{n=0}^{\infty} \frac{(-1)^n}{2n+1} \exp\left[\frac{-D(2n+1)^2\pi^2 t}{4l^2}\right] \tag{1}$$

where D is the K diffusion coefficient. $V_m(t)$ could then be calculated for each $[K]_m(t)$ using the Goldman, Hodgkin and Katz (GHK) equation for Na and K, i.e.,

$$V_m(t) = \frac{RT}{F} \ln \frac{[K]_m(t) + \propto [Na]_o}{[K]_i + \propto [Na]_i} \tag{2}$$

(where $\propto$ is the ratio of Na and K permeability, P_{Na}/P_K). The membrane time constant was short compared to diffusion times (*see Results*), and V_m was considered to be instantaneously set by $[K]_m$.

For some situations it was necessary to treat the membrane as two parallel components with potentials V_S and V_T and conductances G_S and G_T (*see* Fig. 2) and to make K diffusion to component T slower than K diffusion to component S. To estimate the time course

Table 2. Average V_m recorded from preparations before and at least 30 min after a 1-hr soak in a glycerol-Krebs solution[a]

Glycerol concentration (mM)	V_m before treatment (mV) mean ± SE (n)	V_m after treatment (mV) mean ± SE (n)
200	−66.0 ± 3.2 (6)	−51.8 ± 2.8 (17)
300	−61.3 ± 3.5 (14)	−52.6 ± 2.2 (27)
350	−70.1 ± 2.5 (8)	−49.9 ± 3.7 (23)
400	−72.2 ± 1.5 (18)	−35.7 ± 2.9 (44)

[a] The preparations were returned to the normal Krebs solution (solution *A*, Table 1) after the glycerol-Krebs soak and before electrical recording.

of V_m, the simplifying assumption was made that G_S and G_T were constant. V_m is a function of the potentials across each component and

$$V_m = V_S \cdot \frac{G_S}{(G_S + G_T)} + V_T \cdot \frac{G_T}{(G_S + G_T)}. \tag{3}$$

It was convenient to express changes in V_m as $\Delta \bar{V}_m$, where $\Delta \bar{V}_m$ is $[V_m(\infty) - V_m(t)]$. $V_m(\infty)$ is the steady-state V_m after a change in $[K]_0$ and $V_m(t)$ is the V_m at time t after a change in $[K]_0$. Expressions for $V_m(\infty)$, $V_m(t)$ and $\Delta \bar{V}_m$ in terms of V_S, V_T, G_S and G_T were derived from Eq. (3), i.e.,

$$V_m(\infty) = V_S(\infty)\,[G_S/(G_S + G_T)] + V_T(\infty)\,[G_T/(G_S + G_T)] \tag{4}$$

$$V_m(t) = V_S(t)[G_S/(G_S + G_T)] + V_T(t)\,[G_T/(G_S + G_T)] \tag{5}$$

and since

$$\bar{V}_S = [V_S(\infty) - V_S(t)] \text{ and } \bar{V}_T = [V_T(\infty) - V_T(t)],$$

$$\bar{V}_m = \bar{V}_S[G_S/(G_S + G_T)] + \bar{V}_T[G_T/(G_S + G_T)]. \tag{6}$$

The simplifying assumption that G_S and G_T are constant means that values of G_S and G_T obtained by curve-fitting methods have no real meaning. The purpose is simply to show that the data could be fitted by assuming that K_m changed with two different diffusion profiles.

When Cl was used as the principal external anion, the GHK equation for Na, K, and Cl was used to describe the steady-state V_m, i.e.,

$$V_m = \frac{RT}{F} \ln \frac{[K]_0 + \alpha[Na]_0 + \gamma[Cl]_i}{[K]_i + \alpha[Na]_i + \gamma[Cl]_0} \tag{7}$$

where γ is the ratio of K to Cl permeability, P_{Cl}/P_K.

Electrophysiology

V_m was measured with intracellular glass microelectrodes filled with 3 M KCl, and chart records were obtained on a Hewlett Packard 7401 pen recorder. A 3-M KCl salt bridge was used as a reference electrode.

Results

The membrane potential recorded when $[K]_0$ was changed from 3.5 to 50 mM and back to 3.5 mM is shown in Fig. 1. The smaller and slower of the potential changes (Fig 1*A*) was recorded from a fiber in normal (160 mM) $[Cl]_0$ solutions where G_{Cl} was high. The response is contrasted with the potential change recorded in low (8.0 mM) $[Cl]_0$ (Fig 1*B*) where G_{Cl} was presumably low. Low $[Cl]_0$ solutions were used in preference to zero $[Cl]_0$ solutions since the fibers became depolarized after long periods in zero $[Cl]_0$.

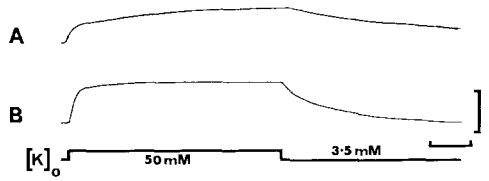

Fig. 1. Continuous record of V_m when $[K]_o$ was changed from 3.5 to 50 to 3.5 mM at times indicated by the line at the bottom of the figure. In *A* the solutions contained 160 mM $[Cl]_o$ (solutions *A* and *B*, Table 1). The steady-state V_m of this fiber in 3.5 mM $[K]_o$ was −68 mV. In *B* the solutions contained 8.0 mM $[Cl]_o$ (solutions *C* and *D*, Table 1). The steady-state V_m of this fiber in 3.5 mM $[K]_o$ was −72 mV. Horizontal calibration: 48 sec; vertical calibration: 40 mV

Low $[Cl]_o$ Solutions

When $[Cl]_0$ is low (as in the experiment shown in Fig. 1*B*) the major membrane conductance is G_K and the change in V_m with a change in $[K]_0$ depends on the rate at which the concentration of K on the outside surface of the membrane changes and on the membrane time constant. The time constant in low $[Cl]_0$ solutions was about 40 msec (G. Carter & A. F. Dulhunty, *unpublished*) which is fast compared to diffusion times (*see* below) and is not rate limiting. The time course of depolarization in 50 mM $[K]_0$ was examined to see whether surface membrane and T-tubule membrane components could be separated.

Depolarization to steady-state V_m. The depolarization when $[K]_0$ was increased from 3.5 to 50 mM has been plotted in Fig. 2. $\Delta\bar{V}_m$ has been plotted on a logarithmic scale to display small slow changes in potential. The initial depolarization is slow (approx. 10 sec) compared with that reported for amphibian fibers (Hodgkin & Horowicz, 1960; Nakajima, Nakajima & Peachey, 1973); however, the time course is consistent with a diffusion profile calculated with an unstirred layer thickness of 170 μm (*see Methods*) and the free solution diffusion coefficient for K. An unstirred layer of 170 μm is reasonable for the surface fibers of bundles still surrounded by connective tissue.

The depolarization plotted in Fig. 2 was slower than the calculated V_m after the first 10 sec, suggesting that there was a delay in diffusion of K to a part of the membrane. In order to fit the whole depolarization the membrane was considered to have two parallel components, shown in Fig 2 (insert), and the diffusion time to each component was varied until the time course of the calculated V_m was close to the recorded V_m. The broken line and the dotted line in Fig. 2 were calculated for each component by methods described in the figure legend. The slowing of $\Delta\bar{V}_T$ (broken line) could be achieved by a 2.6-fold decrease in the diffusion coefficient for K. The solid line in Fig. 2 is the numerical sum of ΔV_S (dotted line) and $\Delta\bar{V}_T$ (broken line). It is apparent that the time course of the recorded depolarization can be described by assuming that K reached the membrane along two different diffusion profiles.

The repolarization with a drop in $[K]_0$ from 50 to 3.5 mM could not be predicted in a simple way. It is probable that repolarization is complicated by restricted diffusion of K away from the fiber and by the behavior of the inward K

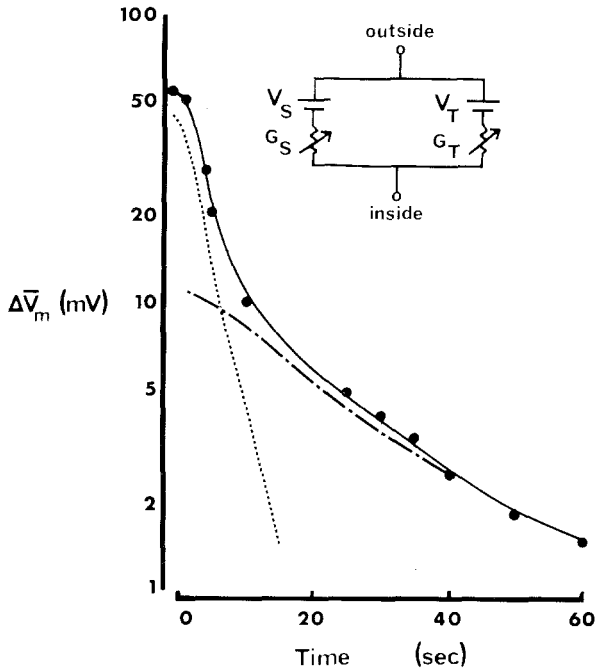

Fig. 2. The time course of the depolarization recorded when $[K]_o$ was changed from 3.5 to 50 mM in low $[Cl]_o$ solutions. $\Delta\bar{V}_m$ (vertical axis; logarithmic scale) is plotted against time in sec ($\Delta\bar{V}_m$ is defined in the *Methods* section). The equivalent circuit (insert) shows two electrically continuous areas of membrane, one with restricted access to the bulk solution having a potential, V_T, and a conductance, G_T, and the other with unrestricted access to the bulk solution having a potential, V_S, and a conductance, G_S. Filled circles: recorded depolarization from a normal fiber. Dotted line: calculated fraction of $\Delta\bar{V}_m$ due to a change in V_S. Broken line: calculated fraction of $\Delta\bar{V}_m$ due to a change in V_T. Continuous line: the numerical sum of the potentials in the dotted line and broken line. The fractions of $\Delta\bar{V}_m$ due to changes in V_S and V_T were calculated with Eqs. (1) to (5) (*see Methods*). The steady-state V_m in 50 mM $[K]_o$ was calculated with Eq. (2) using constants given in Table 3. V_S and V_T were also calculated with Eq. (2) using values of K_m calculated with Eq. (1). The dotted line was calculated from a diffusion profile obtained with $l = 150$ μm and $D = 1.6 \times 10^{-5}$ cm^2 sec^{-2} and scaled to fit the experimental data with $G_S/(G_S + G_T) = 0.82$. The broken line was calculated from a diffusion profile obtained with $l = 150$ μm and $D = 2.4 \times 10^{-6}$ cm^{2}sec^{-2} and scaled to fit the experimental data with $G_T/(G_S + G_T) = 0.18$.

rectifier with changes in $V_m - V_K$. Evidence is presented in the following three sections to show that the slow component of depolarization and the slow repolarization are associated with areas of restricted K diffusion within each fiber and are not diffusion artifacts introduced by flow through the bath or by the large bundles of fibers used.

Glycerol-treated fibers. Glycerol treatment has been shown to effectively interrupt the continuity between the surface membrane and at least 80% of the T-tubule membrane in amphibian skeletal muscle fibers (Eisenberg & Eisenberg, 1968; Franzini-Armstrong, Venosa & Horowicz, 1973). Similar experiments have

not been done in mammalian preparations, but it is reasonable to assume that changes in the V_m response to a change in $[K]_0$ after glycerol-treatment would be associated with changes in the T-system. $\Delta \bar{V}_m$ recorded from a glycerol-treated fiber after a change in $[K]_0$ from 3.5 to 22 mM is shown in Fig. 3 (filled circles). The broken line was calculated by using a single diffusion profile and no slow component was observed. The loss of the slow component after glycerol treatment suggests that it is associated with a normally intact T-system.

Brief exposures to 50 mM $[K]_o$. The analysis of data in Fig. 2 suggested that the K concentration within the restricted area did not change significantly for 10 sec after a change in the bulk $[K]_0$. If this is true then the change in V_m during an increase in $[K]_0$ for 10 sec or less must be due to a change in the potential across the easily accessible area of membrane alone. Figure 4*A* shows the time course of recovery of one fiber exposed to 50 mM $[K]_0$ for different times. The time course of repolarization after 4 and 10 sec in 50 mM $[K]_0$ was consistent with V_m calculated from a single diffusion profile (broken lines; Fig. 4*A*), as described in the figure legend. The longer repolarization after 18 and 120 sec in 50 mM $[K]_0$ could not be simply predicted. The experiment was repeated in glycerol-treated fibers to see whether the slow repolarization could be attributed to K accumulation within the T-tubules. The repolarization of one glycerol-treated fiber after 10, 18, and 120 sec in 22 mM $[K]_0$ is shown in Fig. 4*B*. The time course of repolarization

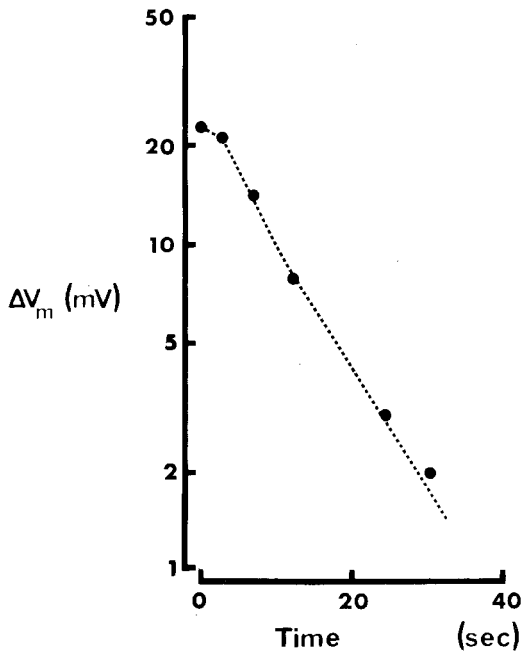

Fig. 3. The time course of the depolarization recorded when $[K]_o$ was changed from 3.5 to 22 mM from a glycerol-treated fiber exposed to low $[Cl]_o$ solutions. $\Delta \bar{V}_m$ is plotted on a logarithmic scale against time in sec. $\Delta \bar{V}_m$ has been defined in *Methods*. The dotted line was calculated with a single diffusion profile using Eqs. (1) and (2) with $l = 220$ μm and $D = 1.6 \times 10^{-5}$cm^2 sec^{-2} [Eq. (1)] and other constants shown in Table 3

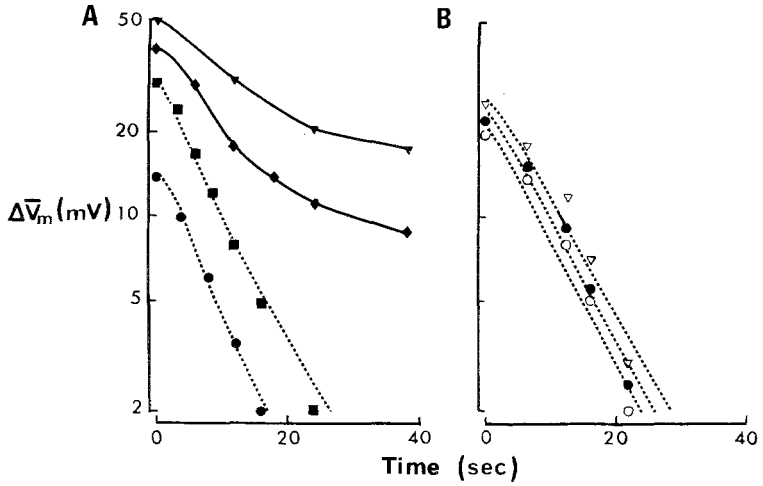

Fig. 4. The time course of repolarization recorded from normal and glycerol-treated fibers when $[K]_o$ was lowered to 3.5 mM after different periods in high $[K]_o$ solutions. All solutions contained low $[Cl]_o$. $\Delta\bar{V}_m$ is plotted on the vertical axis and is defined in *Methods*. (*A*): All records are from one normal fiber which had a resting potential of −74 mV in 3.5 mM $[K]_o$. Circles: recovery from 4 sec in 50 mM $[K]_o$. Squares: recovery from 10 sec in 50 mM $[K]_o$. Diamonds: recovery from 18 sec in 50 mM $[K]_o$. Triangles: recovery from 120 sec in 50 mM $[K]_o$. Broken lines: $\Delta\bar{V}_m$ calculated with Eqs. (1) and (2) (*see Methods*), assuming that K_m was higher after 10 sec than after 4 sec in 50 mM $[K]_o$, as expected from the diffusion profile calculated with constants given below. Constants used were $l = 200$ μm and $D = 1.6 \times 10^{-5}$cm^{2}sec^{-2} and other constants calculated for normal fibers in Table 3. The solid lines were drawn by eye through the experimental points. (*B*): All records were taken from one glycerol-treated fiber which had a resting V_m of −65 mV in 3.5 mM $[K]_o$. Open circles: recovery from 10 sec in 22 mM $[K]_o$. Filled circles: recovery from 140 sec in 22 mM $[K]_o$. Broken lines: $\bar{V}_m$ calculated using Eqs. (1) and (2) (*see Methods*) assuming that K_m was higher after longer periods in 20 mM $[K]_o$, as expected from the diffusion profile calculated with constants given below. Constants used were $l = 220$ μm, $D = 1.6 \times 10^{-5}$cm^{2}sec^{-2} and other constants given in Table 3 for glycerol-treated fibers

was not significantly dependent on exposure time and was consistent with V_m calculated from a single diffusion profile (broken lines, Fig. 4*B*) as described in the figure legend. The slow repolarization after longer exposures in normal fibers (Fig. 4*A*) depends on an intact T-tubule system.

The relation between repolarization time in normal fibers and exposure time is illustrated more clearly in Fig. 5. The 50% repolarization times from several normal fibers are plotted against exposure time (open triangles). The average 50% recovery time was constant for exposure times of 3 to 12 sec, increased with exposure times of 12 sec to 4 min, and was constant for exposures longer than 4 min. The simplest interpretation of the data in Figs. 4*A* and 5 is that recovery from exposure to 50 mM $[K]_0$ for periods of 12 sec or longer is slowed because of the time taken for K diffusion out of the T-tubules. When the period in 50 mM $[K]_0$ is less than 10 sec, K concentration in the T-tubules does not have time to change significantly.

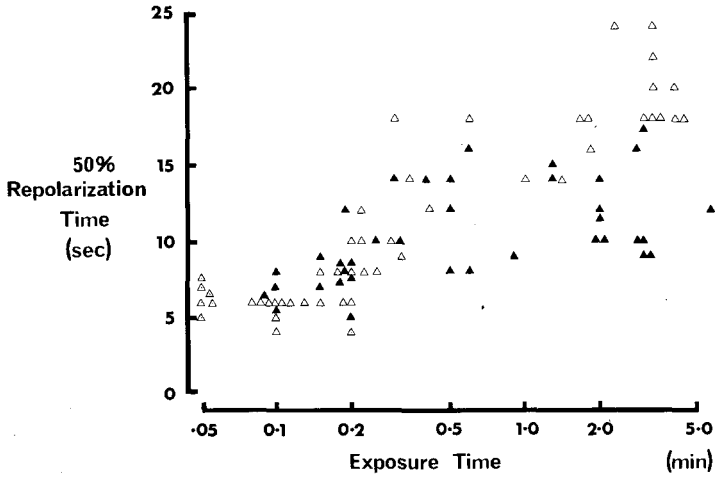

Fig. 5. The recovery of V_m in 3.5 mM $[K]_o$ after different times in 50 mM $[K]_o$. The 50% repolarization times are given on the vertical axis and the duration of exposures to 50 mM $[K]_o$ are shown on the horizontal axis with a logarithmic scale to display the whole range of exposure times. The experiments were done in low $[Cl]_o$ solutions. Open triangles: 50% repolarization in isotonic solutions (solution *C* and *D*, Table 1). Filled triangles: 50% repolarization times in hypertonic solutions (solutions *E* and *F*, Table 1)

Experiments in hypertonic solutions. T-tubule swelling in hypertonic solutions has been demonstrated in electron micrographs of rapidly frozen amphibian fibers (Somlyo, Shuman & Somlyo, 1977) and has also been shown in rat EDL muscle (Davey & O'Brien, 1978). A change in T-tubule geometry could change the rate of K movement through the T-system and the time course of dependent potential changes. The filled triangles in Fig. 5 are the 50% repolarization times recorded from fibers exposed to a 50-mM $[K]_0$ hypertonic solution and then returned to the 3.5-mM $[K]_0$ hypertonic solution (*see* Table 1). The recovery from periods of less than 10 sec in 50 mM $[K]_0$ was the same as in isotonic solutions. Recovery time increased with exposure time when this was between 10 sec and 15 min, although the rate of recovery was faster than it has been in isotonic experiments.

The average time course of depolarization caused by an increase in $[K]_0$ in hypertonic solutions is compared with the time course of depolarization in isotonic solutions in Fig. 6*A*. The two curves can be superimposed for the first 10 sec. At longer times the hypertonic depolarization (filled circles) was faster than the isotonic depolarization (open circles). In contrast to the depolarization, the repolarization (Fig. 6*B*) was faster in hypertonic solutions than in isotonic solutions for its entire time course. The results plotted in Figs. 5 and 6 show that the access of K ions to the area of membrane that depolarized during the first few seconds after an increase in $[K]_0$ was not altered by hypertonic conditions. Access to the restricted area was apparently increased when fibers were soaked in hypertonic solutions.

To recapitulate, the results of brief changes in $[K]_0$ reinforce the idea that there

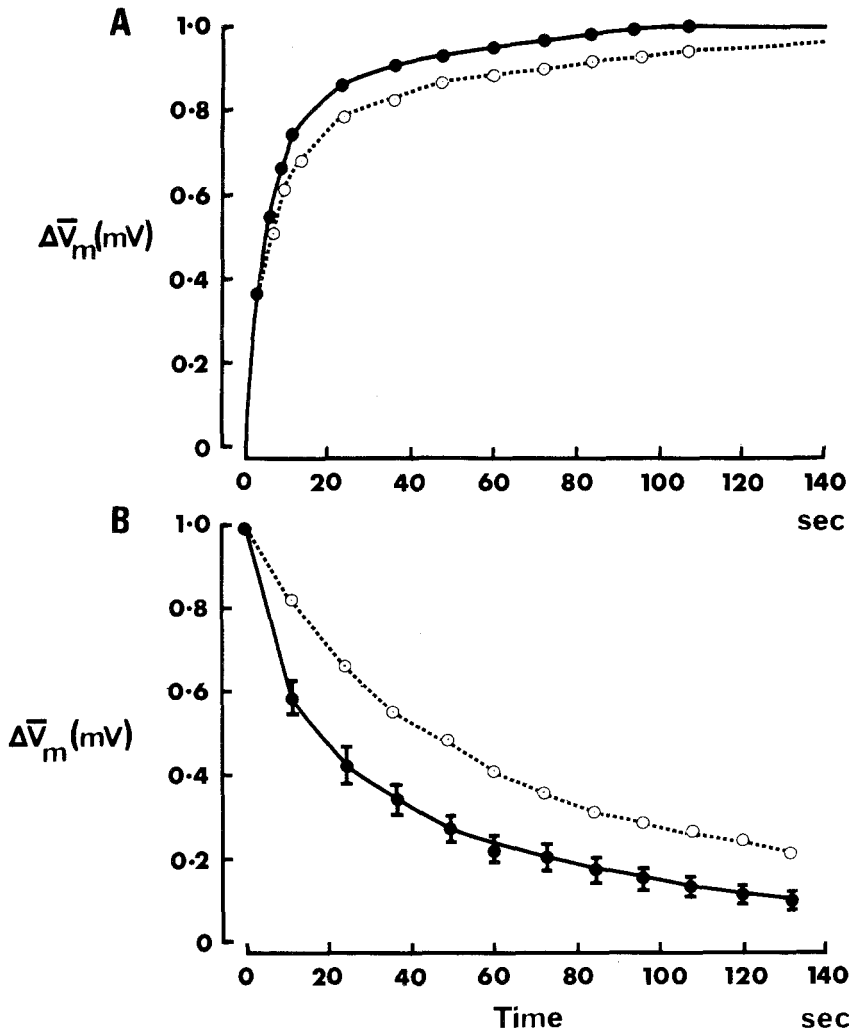

Fig. 6. The average normalized time course of depolarization (3.5 to 50 mM $[K]_o$) and repolarization (50 to 3.5 mM $[K]_o$) of fibers in isotonic and hypertonic, low $[Cl]_o$ solutions. Open circles: isotonic solutions (solutions *C* and *D*, Table 1). Filled circles: hypertonic solutions (solutions *E* and *F*, Table 1). Vertical bars are ± SE where these are greater than the symbol. The continuous lines and broken lines have been drawn through the hypertonic and isotonic data, respectively, by eye. (*A*): Average normalized depolarization of 7 fibers from their steady-state potential in 3.5 mM $[K]_o$ to their steady-state potential in 50 mM $[K]_o$. (*B*): Average normalized repolarization of 6 fibers from their steady-state V_m in 50 mM $[K]_o$ to their steady-state V_m in 3.5 mM $[K]_o$

are two areas of membrane, one with more or less unrestricted access to the bulk solution and one with restricted access to the bulk solution. Results obtained under conditions specifically designed to alter the T-tubules, glycerol treatment and hypertonicity, clearly showed alterations to the components of the potential

changes that had been associated with a restricted space. It seems reasonable to conclude that the restricted space is the T-tubule lumen. In the light of this conclusion it should be emphasized that the lumped treatment of the T-system membrane in Fig. 2 is a gross oversimplification and is meant only to illustrate the difference in diffusion to the two membrane areas. Although relative numbers for surface and T-tubule P_K cannot be obtained from this data, it is apparent that there is a significant fraction of the total P_K in the T-tubule membrane.

The nature of the apparent increase in accessibility of the T-system to $[K]_o$ in hypertonic solutions may not be simply related to the observed T-tubule swelling. Since hypertonic solutions shrink the fiber they must wrinkle the outer membrane, and probably the T-tubules, causing geometrical changes in addition to simple swelling. Until more is known about the total effects of hypertonic solutions on the T-system, the interpretation of the results can be taken no further.

High $[Cl]_o$ Solutions

Relative values for P_{Cl} and P_K are determined in this section by comparing the V_m response to changes in $[K]_o$ in 160 mM $[Cl]_o$ solutions with those in 8.0 mM $[Cl]_o$ solutions. An estimate of the distribution of P_{Cl} on the surface and T-tubule membranes has been obtained from normal and glycerol-treated fibers.

The size of the depolarization caused by an increase in $[K]_o$ in normal (160 mM) $[Cl]_o$ solutions was very variable as shown by the records in Fig. 7 *a-d.* Each record is from a different preparation and is typical of other records in the same preparation. The variability is in contrast to the uniform depolarization recorded in low $[Cl]_o$ solutions: an observation which suggests that the relative values of P_{Cl}/P_K may vary significantly from preparation to preparation. The second significant difference between responses to changes in $[K]_o$ in normal and low $[Cl]_o$ solutions is the time course of the responses. The slow *S*-shaped components of depolarization shown clearly in Fig. 7*B* are unique to the high $[Cl]_o$ responses and are indicative of Cl redistribution (Dulhunty, 1978*a*) and therefore provided useful information about Cl permeability. The time course of repolarization with a decrease in $[K]_o$ (*see*, e.g., Fig. 1) is more sensitive to the presence of high $[Cl]_o$ and hence to changes in $[Cl]_i$ than the time course of depolarization. This point is illustrated in Fig. 7*B* where the 50% repolarization time is 8 min—20 times slower than the repolarization in low $[Cl]_o$ solutions (*see*, e.g., Fig 5). The early time course of Cl influx was therefore studied by looking for the onset of very slow components of repolarization after brief exposures to the high $[K]_o$ solution.

Brief increases in $[K]_o$. V_m recorded during exposure to 50 mM $[K]_o$ in 8 and 160 mM $[Cl]_o$ solutions is shown in Fig 8*A* and *B*, respectively. The time course of repolarization after 10 or 15 sec in 50 mM $[K]_o$ was the same in both solutions (Fig. 8*A*, *a* and *b*, and 8*B*, *a* and *b*). The recovery from 60 sec in 50 mM $[K]_o$ in high $[Cl]_o$ solutions was biphasic (Fig. 8*B*, *c*) and quite different from the monophasic recovery when $[Cl]_o$ was low (Fig 8*A*, *c*). The time course of the early phase of the biphasic repolarization was the same as the monophasic repolarization. The size of the early phase of the biphasic repolarization depended on the time in 50 mM $[K]_o$ and was less than 10% of the repolarization after a 4-min exposure. These ob-

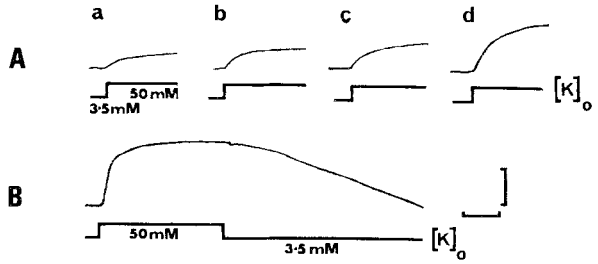

Fig. 7. Records of V_m in 160 mM $[Cl]_o$ solutions during changes in $[K]_o$ from 3.5 to 50 to 3.5 mM (solutions *A* and *B*; Table 1). (*A*): Records from 4 different preparations are shown to demonstrate the variability of the response to a change in $[K]_o$ from 3.5 to 50 mM (indicated on the lines beneath each trace). Vertical calibration: 20 mV, horizontal calibration: 24 sec. (*B*): A continuous record from one preparation exposed to 50 mM $[K]_o$ for 6.5 min (indicated beneath the record). Vertical calibration: 20 mV, horizontal calibration: 2 min

servations are consistent with the Cl redistribution hypothesis if inward K rectification is operative. A reduction in $[K]_o$ would "turn off" G_K and V_m would be effectively set by V_{Cl}. V_{Cl} is more positive than normal after Cl influx, and its exact value depends on the amount of Cl influx which must be less for briefer exposures to 50 mM $[K]_o$. Since V_m returned quickly to its resting value in 3.5 mM $[K]_o$, after 10 and 15 sec in 50 mM $[K]_o$ (Fig 8*B*, *a* and *b*), it is reasonable to conclude that very little Cl influx occurs in the first 10 to 15 sec in 50 mM $[K]_o$. The bulk Cl influx is between 15 sec and 4 min in 50 mM $[K]_o$.

The apparent delay of 10 to 15 sec between the change in bulk $[K]_o$ and significant Cl redistribution suggests that Cl redistribution may depend on K diffusion into the T-tubules. If T-tubule G_{Cl} was much higher than surface G_{Cl} then Cl influx would not begin until the T-tubule membrane began to depolarize. The importance of the T-system in Cl redistribution was assessed by repeating the experiment in glycerol-treated fibers.

Glycerol-treated fibers in high $[Cl]_o$ solutions. Two records from glycerol-treated fibers exposed to 50 mM $[K]_o$ in 160 mM $[Cl]_o$ solutions are shown in Fig. 8*C* (*b* and *c*). Both records look very like records from normal fibers in 8 mM $[Cl]_o$ (Fig. 8*A*): a similarity implying that G_{Cl} is low in glycerol-treated fibers. Repolarization after 7 min in 50 mM $[K]_o$ (160 mM $[Cl]_o$) was biphasic (Fig. 7*D*). Cl redistribution would proceed slowly if there was a small but finite G_{Cl} on the surface membrane.

Responses to changes in $[Cl]_o$. The reduction in G_{Cl} after glycerol-treatment is dramatically illustrated by the response to changes in $[Cl]_o$ in normal and glycerol-treated fibers shown in Fig 9. The normal response to a change in $[Cl]_o$ is an initial potential change which is followed by a slow potential change, of opposite sign, as $[Cl]_i$ changes. In the records shown in Fig. 9 $[Cl]_o$ was changed every 1 to 1.5 min and only the initial potential changes are displayed. The initial potential change was greater in conditions of low $[Cl]_i$ and so preparations were soaked for 15 min in O$[Cl]_o$ before the records shown in Fig. 9 were obtained. The change in V_m was always smaller than expected from considerations of the high G_{Cl} and of V_m - V_{Cl}. This may have been due to the distribution of the T-system across the

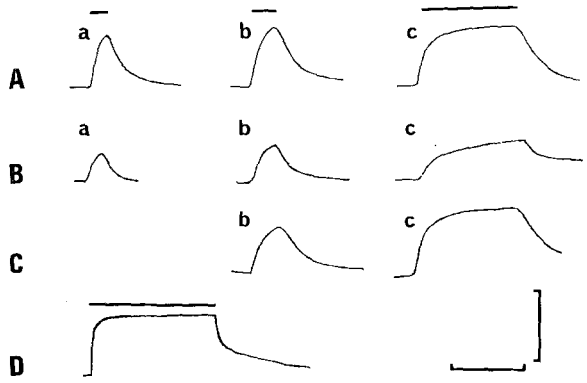

Fig. 8. Continuous records of V_m from normal fibers in 8 mM $[Cl]_o$ solutions (*A*) and 160 mM $[Cl]_o$ solutions (*B*) and glycerol-treated fibers in 160 mM $[Cl]_o$ solutions (*C* and *D*) exposed to 50 mM $[K]_o$ for times indicated by the bars above each trace. In *A*, records from normal fibers in low $[Cl]_o$ solutions are shown. *a*: 12-sec exposure (V_m in 3.5 mM $[K]_o$ was −70 mV); *b*: 20-sec exposure (V_m in 3.5 mM $[K]_o$ was −75 mV); *c*: 70-sec exposure (V_m in 3.5 mM $[K]_o$ was −72 mV). In *B*, records from normal fibers in high $[Cl]_o$ solutions are shown. *a*: 12-sec exposure (V_m in 3.5 mM $[K]_o$ was −65 mV); *b*: 20-sec exposure (V_m in 3.5 mM $[K]_o$ was −69 mV); *c*: 70-sec exposure (V_m in 3.5 mM $[K]_o$ was −68 mV). In *C*, records from glycerol-treated fibers in high $[Cl]_o$ solutions are shown. No record of a 12-sec exposure was obtained. *b*: 20-sec exposure (V_m in 3.5 mM $[K]_o$ was −70 mV), *c*: 70-sec exposure (V_m in 3.5 mM $[K]_o$ was −65 mV). In *D*, a record of a glycerol-treated fiber in 160 mM $[Cl]_o$ exposed to 50 mM $[K]_o$ for 6.5 min is shown. (V_m in 3.5 mM $[K]_o$ was −62 mV). Horizontal calibration: 48 sec for *A*, *B*, and *C*, and 4 min for *D*; vertical calibration: 40 mV

fiber cross-section. Using the initial depolarization in Fig. 9*A* as an example, it could be argued that the depolarization and subsequent hyperpolarization took place at slightly different times on the exterior surface and along the T-tubule membranes so that parts of the membrane were in fact hyperpolarized at the peak of the depolarization. Although the initial change in membrane potential in normal fibers was less than the sum of surface and T-tubule membrane potential changes, the reduction in the response after glycerol treatment is obvious in Fig. 9*B*. The residual response in the glycerol-treated fibers was only marginally larger than the changes in the asymmetry potential shown in Fig. 9*C*. The G_{Cl} of the surface membrane must be very small.

K and Cl permeability ratio. The relative P_{Cl} and P_K of normal and glycerol-treated fibers was calculated with Eq. (2) (at $t = \infty$) and Eq. (7) (*see Methods*) applied simultaneously to the bracketed average V_m values listed in Table 3 (column 5). Steady-state V_m values are given for 8 mM $[Cl]_o$ solutions and for the 3.5 mM $[K]_o$, 160 mM $[Cl]_o$ solutions. The V_m listed for 50 mM $[K]_o$, 160 mM $[Cl]_o$ solutions was recorded 40 sec after the change from 3.5 mM $[K]_o$ to 50 mM $[K]_o$. The steady-state V_m could not be used in this solution because of an unknown amount of Cl redistribution. The change in V_m due to a change in $[K]_o$ was 95% complete after 40 sec (e.g., Fig. 2). The depolarizing effect of a small increase in $[Cl]_i$ after 40 sec meant that V_m at this time was probably very close to the steady-state po-

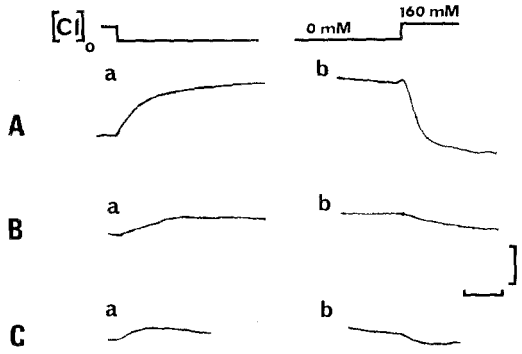

Fig. 9. Continuous records of V_m in 3.5 mM $[K]_o$ during changes in $[Cl]_o$. Fibers were soaked in zero $[Cl]_o$ solutions for 15 min, and then $[Cl]_o$ was changed repetitively from 0 to 160 to 0 mM, as indicated by the top line in the figure. In *A*, intracellular records taken from fibers in a normal preparation are shown. In *B*, intracellular records from fibers of the same preparation after glycerol treatment are shown. In *C*, the changes in asymmetry potential between the reference electrode (3-M KCl salt bridge) and the microelectrode buried deeply in the preparation but located extracellularly are shown. This position of the microelectrode was chosen to best represent the intracellular situation in a surface fiber where there would be a delay between changes in bulk $[Cl]_o$ and changes in the intracellular ion concentrations. Horizontal calibration: 24 sec; vertical calibration: 10 mV

tential that would have been reached if there had not been any Cl redistribution. A second assumption was made that $\gamma[Cl]_o$ and $\gamma[Cl]_i$ were numerically insignificant in 8.0 mM $[Cl]_o$ solutions. This assumption was necessary because $[Cl]_i$ must change with $[Cl]_o$ (Dulhunty, 1978*a*), and so the GHK equation for Na, K, and Cl [Eq. (7)] could not be simultaneously used to solve for the four unknown parameters (*see* right hand side of Table 3). Values for $[K]_i$ and P_{Na}/P_K were calculated with Eq. (2) applied to the bracketed low $[Cl]_o$ data, and these values were used in Eq. (7) to calculate $[Cl]_i$ and P_{Cl}/P_K from the bracketed high $[Cl]_o$ data. $[Na]_i$ was assumed to be 40 mM in each case; however, the term containing $[Na]_i$ is numerically insignificant, and the exact value used is not important.

The calculated values for $[K]_i$, $[Cl]_i$, P_{Na}/P_K and P_{Cl}/P_K are given on the right hand side of Table 3. Confidence in this form of analysis was enhanced by the fact that values calculated for normal fibers are very similar to values calculated from flux measurements and direct measurement of $[K]_i$ (Lipicky & and Bryant, 1966). A significant reduction in P_{Cl}/P_K as well as increases in $[K]_i$, $[Cl]_i$, and $\propto$ are indicated after glycerol treatment. P_{Cl}/P_K can also be calculated from V_m measurements in glycerol-treated fibers by assuming that $[K]_i$, $[Cl]_i$, and $\propto$ are the same as in normal fibers and the steady-state depolarization of the fibers ignored. In this case P_{Cl}/P_K is 0.74. In either case it must be concluded that Cl permeability is significantly less after glycerol treatment.

The apparent increase in $[K]_i$ and $[Cl]_i$ after glycerol treatment (Table 3) is interesting. $[K]_i$ measured in aged glycerol-treated amphibian fibers is less than normal (Henderson, 1970), or normal (Venosa & Horowicz, 1973). No similar data is available for mammalian fibers, and the experiments shown in Table 3

Table 3. Calculation of $[K]_i$, $[Cl]_i$, P_{Na}/P_K and P_{Cl}/P_K from average V_m data obtained from normal and glycerol-treated fibers using GHK equations as outlined in the text

	External ion concentrations				Calculated parameters			
	$[K]_o$	$[Na]_o$ (mM)	$[Cl]_o$	$V_m \pm$ SE (n) (mV)	$[K_i$	$[Cl]_i$ (mM)	P_{Na}/P_K α	P_{Cl}/P_k γ
Normal fibers	3.5	84	8	78.3 ± 0.8 (7)	150		0.058	
	50	37.5	8	29.7 ± 0.5 (7)				
	3.5	150	160	70.5 ± 1.5 (15)		12.6		4.5
	50	103	160	55.1 ± 1.5 (15)				
Glycerol-treated fibers	3.5	84	8	69.7 ± 1.2 (6)	209		0.15	
	50	37.5	8	36.4 ± 0.9 (6)				
	3.5	150	160	66.3 ± 1.1 (11)		20.22		0.28
	50	103	160	38.2 ± 1.7 (11)				

were done in freshly glycerol-treated fibers. Such an increase in $[K]_i$ and $[Cl]_i$ might be expected if the K and Cl pump sites were located on the surface membrane, but the leakage sites for the ions distributed over both the surface and T-tubule membranes. The rate of ion accumulation would not be significantly altered by detubulation, although the rate of ion leakage from the fiber would be less. There is evidence (Venosa & Horowicz, 1973), that active Na efflux from frog semitendinosus fibers is not altered by glycerol treatment and hence that the site of active Na/K exchange is the surface membrane.

Discussion

The specific conductance and/or permeability of the surface and T-tubule membranes must be known before a comparison of "channel" density on the two membranes can be made. Specific T-tubule permeability ratios cannot be calculated for either the diaphragm or sternomastoid fibers since the areas of T-tubule membrane are not known. A possible range of T-tubule membrane areas can be estimated from other evidence. T-tubule membrane areas of 4 times the surface membrane area have been reported for guinea pig soleus fibers (Eisenberg, Kuda & Peter, 1974), and larger areas are indicated in rat EDL fibers by results presented by Davey and O'Brien (1978). The analysis of data in Table 3 suggests that P_{Cl}/P_K is 16 times greater in normal fibers than in glycerol-treated fibers. In the worst case (*see Results*) the calculated P_{Cl}/P_K of normal fibers may be reduced to only 6 times that of glycerol-treated fibers. In this case it would be difficult to say that the specific Cl permeability of the T-tubule membrane was greater than that of the surface membrane. However, an additional consideration must be the degree of detubulation of the glycerol-treated fibers. Detubulation is never 100%

complete in amphibian fibers (Eisenberg & Eisenberg, 1968; Franzini-Armstrong *et al.*, 1973), and it is unlikely that it is 100% complete in mammalian fibers (G. Carter, D.F. Davey & A.F. Dulhunty, *unpublished*). With this consideration it seems reasonable to suggest that the specific P_{Cl}/P_K of the T-tubule membrane is greater than that of the surface membrane.

Two models have been presented to explain the nonuniformity of P_{Cl} over the plasmalemma of frog skeletal muscle fibers. The first is that the distribution of Cl "channels" is uniform but that there is a net negative charge within the T-tubule lumen that restricts Cl entry (Fatt, 1964; Rappoport, Peachey & Goldstein, 1969). The fact that the specific P_{Cl} of mammalian T-tubule membrane is greater than the specific P_{Cl} of the surface membrane means that this model cannot be applied to mammalian muscle for reasons given in the introduction. The second possibility is that there are different "channel" densities on the two membranes (Eisenberg & Gage, 1969). Thus the mammalian T-tubule membrane would have more Cl "channels" than the surface membrane. In support of such a hypothesis the surface membrane has been found to be structurally quite different from the T-tubule membrane in freeze-fracture replicas (Franzini-Armstrong, 1974). The selectivity of an area of membrane for a "channel" could depend on specific interactions between the membrane lipid and the "channel" molecule. Such interactions need only involve a few amino-acid residues which are subject to genetic alteration. The hypothesis requires that there be differences in the lipid of the exterior surface and T-tubule membranes. The T-tubules maintain a small diameter cylindrical structure so that the lipid composition may well be different from that forming the essentially flat surface membrane.

There are obvious advantages to the T-tubule membrane having a high P_{Cl} since this would reduce the outward K current during the action potential and reduce the tendency for K accumulation in the T-tubules. A causal relation between T-tubule K accumulation and myotonic activity has been demonstrated in goats with a genetic deficit in G_{Cl} (Adrian & Bryant, 1974). Following the same argument, the low T-tubule G_{Cl} in amphibian fibers should mean that repetitive activity would cause more T-tubule K accumulation in these fibers than it would in mammalian fibers. Indeed, Hanson (1974) presented data indicating that the late after-potential, which reflects T-tubule K accumulation (Freygang *et al.*, 1964; Gage & Eisenberg, 1969), is greater in frog muscle than in rat muscle and is virtually nonexistent in human muscle. The early after-potential, which probably arises in the T-system (Gage & Eisenberg, 1969; Adrian & Peachey, 1973), is much more affected by repetitive stimulation in frog muscle than in either rat or human muscle. Thus phylogenetic changes in the distribution of P_{Cl} mean that mammalian muscle fibers are better able to cope with long periods of repetitive activity.

I am grateful to Dr. P.H. Barry, Dr. D. Davey, and Professor P.W. Gage for their helpful discussion during preparation of the manuscript. I am also grateful to Miss M. Dlutowski for the technical assistance and to Mrs. J. Putnam, for typing the manuscript.

The work was supported by Grants from the Muscular Dystrophy Association of America and the Australian Research Grants Committee.

References

Adrian, R.H., Bryant, S.H. 1974. On the repetitive discharge in myotonic muscle fibres. *J. Physiol. (London)* **240:**505

Adrian, R.H., Chandler, W.K., Hodgkin, A.L. 1970. Voltage clamp experiments in striated muscle fibres. *J. Physiol. (London)* **208:**607

Adrian, R.H., Peachey, L.D. 1973. Reconstruction of the action potential of frog sartorius muscle. *J. Physiol. (London)* **235:**103

Crank, J. 1975. Mathematics of Diffusion. (2nd ed.) Clarendon Press, Oxford

Davey, D., O'Brien, G. 1978. The sarcoplasmic reticulum and T-system of rat extensor *digitorum longus* muscles exposed to hypertonic solutions. *Aust. J. Exp. Biol. Med. Sci. (in press)*

Dulhunty, A.F. 1978*a*. The dependence of membrane potential on extracellular chloride concentration in mammalian skeletal muscle fibres. *J. Physiol. (London)* **276:**67

Dulhunty, A.F. 1978*b*. Potassium and chloride permeability of normal and glycerol-treated mammalian skeletal muscle fibers. *Proc. Aust. Physiol. Pharmacol. Soc.* **10:**24

Eisenberg, B.R., Eisenberg, R.S. 1968. Selective disruption of the sarcotubular system in frog sartorius muscle. *J. Cell. Biol.* **39:**451

Eisenberg, B.R., Kuda, A.M., Peter, J.B. 1974. Stereological analysis of mammalian skeletal muscle. *J. cell. Biol.* **60:**732

Eisenberg, R.S., Gage, P.W. 1969. Ionic conductances of the surface of transverse tubular membranes of frog sartorius fibres. *J. Gen. Physiol.* **53:**279

Eisenberg, R.S., Howell, J.N., Vaughan, P.D. 1971. The maintenance of resting potentials in glycerol treated muscle fibres. *J. Physiol. (London)* **215:**95

Fatt, P. 1964. An analysis of the transverse electrical impedance of striated muscles. *Proc. R. Soc. B.* **159:**606

Franzini-Armstrong, C. 1974. Membrane particles and transmission at the triad. *Fed. Proc.* **34(5):**1382

Franzini-Armstrong, C., Venosa, R.A., Horowicz, P. 1973. Morphology and accessibility of the transverse tubular system in frog sartoriuis muscle after glycerol treatment. *J. Membrane Biol.* **14:**179

Freygang, W.H., Goldstein, D.A., Hellam, D.C., Peachey, L.D. 1964. The relation between the late after potential and the size of the transverse tubular system of frog muscle. *J. Gen. Physiol.* **48:**235

Gage, P.W., Eisenberg, R.S. 1969. Action potentials, after potentials, and excitation-contraction coupling in frog sartorius fibers without transverse tubules. *J. Gen. Physiol.* **53:**298

Hanson, J. 1974. Effects of repetitive stimulation on membrane potentials and twitch in human and rat intercostal muscle fibers. *Acta Physiol. Scand.* **92(2):**238

Henderson, E.G. 1970. Potassium exchange and afterpotentials in frog sartorius muscles treated with glycerol. *J. Gen. Physiol.* **56:**693

Hodgkin, A.L., Horowicz, P. 1960. The effect of sudden changes in ionic concentrations on the membrane potential of single muscle fibres. *J. Physiol. (London)* **153:**370

Lipicky, R.J., Bryant, S.H. 1966. Sodium, potassium and chloride fluxes in intercostal muscle from normal goats and goats with hereditary myotonia. *J. Gen. Physiol.* **50:**89

Nakajima, S., Nakajima, Y., Peachey, L.D. 1973. Speed of repolarization and morphology of glycerol-treated muscle fibers. *J. Physiol. (London)* **234:**449

Palade, P.T., Barchi, R.L. 1977. Characteristics of the chloride conductance in muscle fibers of rat diaphragm. *J. Gen. Physiol.* **69:**325

Rappoport, S.I., Peachey, L.D., Goldstein, D.A. 1969. Swelling of the transverse tubular system in frog sartorius. *J. Gen. Physiol.* **54:**166

Somlyo, A.V., Shuman, H., Somylo, A.P. 1977. Elemental distribution in striated muscle and the effects of hypertonicity electron probe analysis of cryo sections. *J. Cell. Biol.* **74:**828

Venosa, R.A., Horowicz, P. 1973. Effects on sodium efflux of treating frog sartorius muscles with hypertonic glycerol solutions. *J. Membrane Biol.* **14:**33